Failure Mechanisms in Explosively Driven Power Supplies

by R. E. Setchell, J. D. Keck, S. T. Montgomery, M. U. Anderson, and D. E. Cox

Motivation—In explosively driven power supplies, voltages and currents are generated through shock-induced depoling of ferroelectric ceramic elements. The shock wave is generated by detonating an adjacent explosive charge, resulting in a diverging, attenuating wave structure propagating through the encapsulated volume containing the ceramic elements. Acceptance testing of the material used for high voltage generation (PZT 95/5) is limited by high-voltage breakdowns that occur late in time as the wave propagates through a test sample, particularly at cold temperatures. A fundamental understanding of this and other possible failure mechanisms could have a significant impact on material acceptance rates, design margins, and overall power supply reliability.

Accomplishment—Two developments were necessary in order to obtain new insights into power supply failure mechanisms. The first involved gas-gun techniques for generating diverging, attenuating wave structures similar to those generated by the detonation of a small explosive charge. A number of non-planar impactor designs at various impact velocities were examined in order to establish conditions that mimicked wave properties measured in actual power supplies. The second development was to divide the ground electrode of a poled PZT 95/5 bar into as many as five isolated segments along the bar length. During shock motion along the bar, currents flowing between each segment and ground are monitored independently using current-viewing resistors (CVRs). A resistive load is used to generate an appropriate electric field in the PZT 95/5 bar. A schematic of this experimental configuration is shown in Fig. 1, and typical currents recorded during an experiment are shown in Fig. 2. During shock propagation, the individual CVRs record the depoling current, the load-resistor current producing an electric field, and the charging currents on each segment reflecting their capacitance. In the experiment summarized in Fig. 2, a failure event occurs as the shock is passing from the fourth to the fifth segment. Current spikes indicate the onset of internal conduction in the first segment, which has experienced compression by the highest-strength shock followed by unloading to near-ambient pressures. A conduction "front" appears to be propagating into subsequent segments later in time. Figures 3 and 4 show the initial temperature dependence of other properties that can be obtained from these information-rich experiments.

Significance—These experiments are revealing previously unknown details of failure mechanisms-the "where" and "what," rather than just the "when." By combining these details with the results of extensive studies of PZT 95/5 properties under one-dimensional shock loading we have conducted in recent years, we are able to establish reasonable descriptions of failure processes. We now believe that the failure event shown in Fig. 2 results from PZT 95/5 material near the front of the bar being compressed well beyond its threshold for dynamic yielding, resulting in significant material damage, followed by a loss of dielectric strength during subsequent unloading due to the unsupported shock structure. Shock properties at cold temperatures exacerbate these processes. With such understanding, design parameters now can be critically examined with the goal of minimizing the probability of failures.

Sponsors for various phases of this work include: Nuclear Weapons/Advanced Design and Production Technologies (ADAPT)
Contact: Robert E. Setchell, Nanostructures & Advanced Materials Chemistry, Dept. 1122
Phone: (505) 844-3847, Fax: (505) 844-4045, E-mail: resetch@sandia.gov

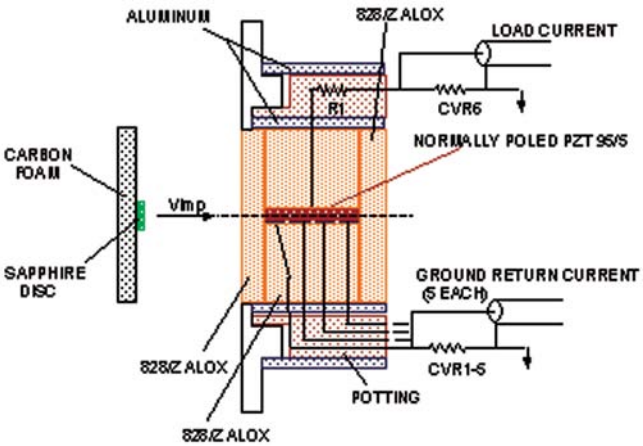

Figure 1. Configuration for "segmented bar" gas gun experiments. Non-planar impact results in a diverging, attenuating shock wave similar to that produced by an explosive charge.

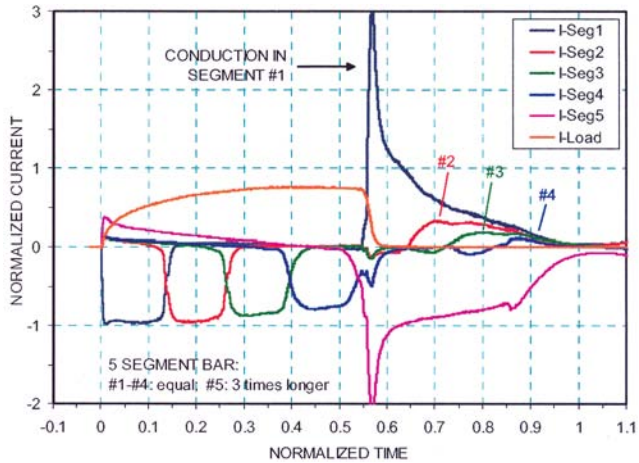

Figure 2. Currents recorded during an experiment at room temperature. The shock wave is entering the last segment when a conductive failure occurs in the first segment.

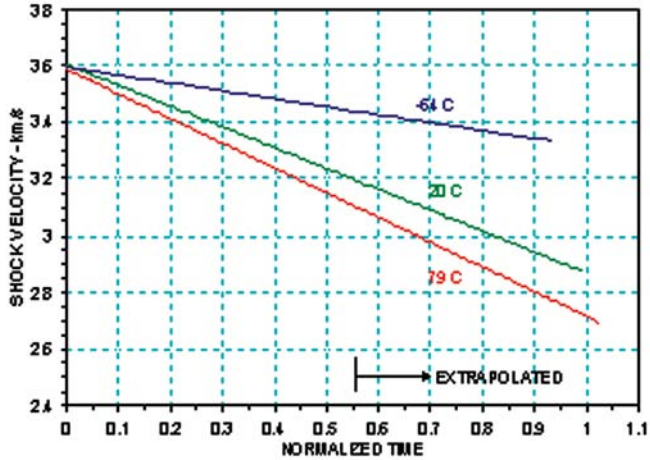

Figure 3. Shock velocity within the PZT 95/5 bars for different initial temperatures. Velocity values are determined from a distance-time fit based on the individual segment currents.

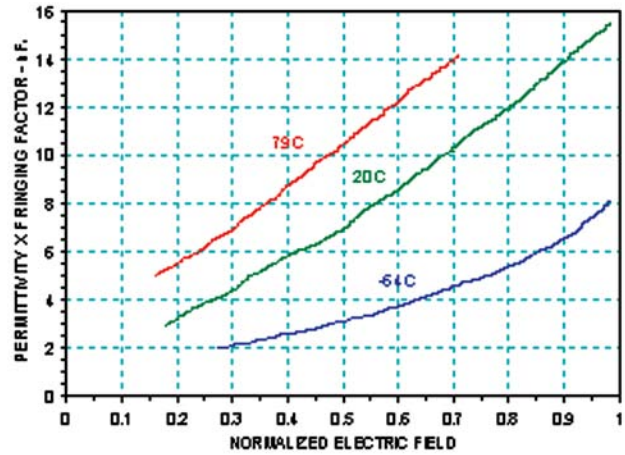

Figure 4. Dielectric properties of the final bar segment prior to shock wave arrival. The trend with initial temperature is consistent with the trend in small-signal measurements of dielectric constant.